Textile & Leather Review

ISSN 2623-6281| www.tlr-journal.com | 10.31881/TLR

Acoustic Performance of Gradient Density Nonwoven Textiles for Sound Absorption

Fei Mo

How to cite: Mo F. Acoustic Performance of Gradient Density Nonwoven Textiles for Sound Absorption. Textile & Leather Review. 2025; 8:1107-1123. https://doi.org/10.31881/TLR.2025.1107

How to link: https://doi.org/10.31881/TLR.2025.1107

Published: 26 December 2025

Acoustic Performance of Gradient Density Nonwoven Textiles for Sound Absorption

Fei MO
School of Art, Shangluo University, Shangluo 726000, Shaanxi, China
mf8602lxl1988@163.com

Article
https://doi.org/10.31881/TLR.2025.1107
Received 12 September 2025; Accepted 15 October 2025; Published 26 December 2025

ABSTRACT

This study presents the design, fabrication, and performance optimization of a high-performance acoustic textile engineered from a nonwoven composite structure, with the aim of enhancing sound absorption in critical acoustic environments. A monolithic composite with a continuous density gradient was fabricated using polyester (PET) staple fibers of two distinct linear densities: 3.3 dtex (3 denier) and 16.7 dtex (15 denier). Hereafter, we use denier consistently, and the abbreviations 3D/15D refer to 3 denier and 15 denier, respectively (conversion: 1 dtex ≈ 0.9 denier). The textile manufacturing process involved industrial carding to form fibrous webs, strategic layering of 100% 15D, a 50/50 blend, and 100% 3D PET webs, followed by mechanical consolidation via a needle-punching process. This technique creates a unique micro-to-macro fibrous architecture, transitioning from a low-density, coarse-fiber sound-incident layer to a high-density, fine-fiber back layer. This engineered structure establishes a gradient in airflow resistance, creating an improved gradient for acoustic impedance and thereby minimizing surface reflection under normal incidence. The influence of key structural parameters, including area density (1,200–1,800 g/m²) and thickness (15–25 mm), was systematically investigated, with the sound absorption coefficient measured according to ASTM E1050. An optimized composite textile (1,600 g/m², 20 mm) demonstrated superior absorption, achieving a Noise Reduction Coefficient (NRC) of 0.75 (based on normal incidence data), significantly outperforming a uniform control sample. This work validates a microstructural engineering strategy for developing advanced functional nonwoven textiles.

KEYWORDS
nonwoven textiles, acoustic properties, needle-punching, polyester fibers

INTRODUCTION

The intrinsic quality of a musical performance is inextricably linked to the acoustic character of the space in which it occurs. In architectural acoustics, spaces designed for music—such as concert halls, opera houses, recording studios, and rehearsal rooms—are considered among the most demanding environments to design [1,2]. The primary objective is to create a sound field that enhances the musical experience, characterized by desirable attributes like appropriate reverberation, good clarity, spaciousness, and the absence of acoustic defects [1,3]. Uncontrolled sound reflections from acoustically reflective surfaces (walls, ceilings, and floors) can lead to a host of problems, including excessive reverberation time (RT60), which masks temporal details in music; standing waves, which cause uneven sound distribution; and flutter echoes, which introduce a disturbing ringing coloration [4]. Consequently, the strategic application of sound-absorbing materials is an indispensable tool for the acoustic engineer to sculpt the room's response and achieve the desired auditory ambiance [4].

For decades, the field of acoustic treatment has been dominated by traditional materials like fiberglass, mineral wool, and open-cell polyurethane foams [5]. While acoustically effective, these materials are not without drawbacks. Concerns regarding the inhalation of fine fibers, the use of formaldehyde-based binders, limited aesthetic options, and difficulties in installation and maintenance have spurred significant research into alternative solutions [6]. In this context, fibrous textile materials, and nonwovens in particular, have garnered considerable attention as a promising class of porous sound absorbers. Nonwovens offer a unique constellation of properties: they are lightweight, flexible, durable, and can be engineered from a wide range of synthetic and natural fibers, including recycled materials, thus offering sustainability benefits [7,8]. Aesthetically, they can be produced in various colors and textures, allowing for seamless integration into interior design concepts [9].

The fundamental mechanism of sound absorption in porous nonwoven materials is the irreversible conversion of acoustic energy into low-grade heat. As a sound wave impinges upon and propagates through the tortuous, interconnected pore network of the fibrous structure, it forces the air within the pores to oscillate [10]. This oscillation gives rise to energy loss through two primary physical processes: viscous friction at the interface between the oscillating air and the stationary fibers, and thermal relaxation due to localized compression and rarefaction of the air, leading to heat exchange with the fibers [10]. The efficacy of these energy dissipation mechanisms is governed by the material's intrinsic physical properties, principally its airflow resistance, porosity, and tortuosity. These macroscopic properties are, in turn, a direct consequence of the material's microstructure: fiber diameter, fiber orientation, bulk density, and overall thickness.

Much of the existing research on nonwoven sound absorbers has focused on homogeneous, single-layer structures. While effective in the mid-to-high frequency range, these materials often struggle to provide significant absorption at lower frequencies unless a substantial thickness or a large air gap behind the material is employed, which is often architecturally undesirable [11,12]. To overcome this limitation, researchers have explored multi-layer and composite structures. By combining layers with different densities or fiber types, it is possible to broaden the absorption bandwidth. However, such discrete multi-layer systems can suffer from impedance mismatches at the layer interfaces, leading to internal reflections that can compromise overall performance [12,13]. This study seeks to advance this field by proposing and systematically investigating a more sophisticated structural concept: a nonwoven composite with a continuous density gradient.

The core hypothesis of this research is that a monolithic structure with a carefully engineered gradient of fiber density—from a highly porous, low-density front layer to a dense, fine-fiber back layer—can achieve a more optimal impedance gradient. The low-density frontal region is designed to act as an impedance-matching layer, minimizing the initial reflection of incident sound waves and facilitating their penetration into the material's core. As the wave travels deeper, it encounters a progressively denser fibrous network, resulting in a gradual and highly efficient dissipation of its energy. This approach avoids the sharp interfaces of multi-layer systems and aims to maximize energy loss throughout the material's entire thickness. This study focuses specifically on polyester (PET) fibers due to their widespread availability and processability. By systematically fabricating and testing a series of gradient composites, varying key manufacturing parameters like area density and thickness, this work aims to establish a clear structure-property relationship. The ultimate goal is to provide a detailed, data-driven understanding of how a gradient structure can be optimized to maximize broadband absorption efficiency, thereby offering a potential pathway for developing advanced materials suitable for high-fidelity music environments.

MATERIALS AND METHODS

Materials Selection and Rationale

The selection of raw materials is a critical first step in engineering a functional nonwoven composite. For this study, PET staple fibers were chosen as the exclusive fibrous component. PET is a semi-crystalline thermoplastic polymer widely used in the textile industry, and its selection was based on several key criteria. First, PET fibers exhibit excellent intrinsic mechanical properties, including high tensile strength and resilience, which translate into a durable and structurally stable final product capable of withstanding handling and installation stresses. Second, PET is inherently hydrophobic, demonstrating low moisture regain. This characteristic is crucial for acoustic applications, as moisture absorption can significantly alter the material's density and pore structure, thereby degrading its sound absorption performance over time. Third, PET fibers are available in a wide range of linear densities (deniers) and are readily processable using standard nonwoven manufacturing techniques such as carding and needle-punching.

To construct the gradient structure, two distinct types of PET staple fibers were sourced: 3 denier (3D; ≈3 dtex) and 15 denier (15D; ≈17 dtex); we use denier throughout, and 3D/15D denote 3 denier/15 denier, respectively. Both fiber types had a consistent staple length of 64 mm to ensure uniform processing behavior. The fine 3D fibers, with a higher surface area per unit mass, are highly effective at creating a dense network with high airflow resistance, ideal for maximizing viscous losses. Conversely, the coarse 15D fibers are better suited for forming a lofty, highly porous structure with low airflow resistance, making them ideal for the sound-incident impedance-matching layer.

Fabrication of Gradient Density Nonwoven Composites

The fabrication process was meticulously designed to translate the conceptual gradient structure into a physical material. The process involved two main stages: multilayer web formation and mechanical bonding via needle-punching.

- **Web Formation:** The initial step was the creation of fibrous webs using an industrial-scale carding machine. The carding process disentangles clumps of staple fibers and aligns them into a continuous, uniform web. Three distinct types of webs were produced: a web of 100% 15D PET fibers, a web of 100% 3D PET fibers, and a transitional web formed from a 50/50 blend of 15D and 3D fibers. To create the precursor batt for the gradient composite, these webs were layered onto a conveyor in a specific sequence using a cross-lapper to achieve the target area density and build up thickness. The layering sequence was as follows: a bottom layer of 100% 3D PET, a middle layer of the 50/50 blend, and a top layer of 100% 15D PET. The relative mass proportions of these layers were controlled at approximately 40% (15D layer), 20% (blend layer), and 40% (3D layer) to ensure a smooth transition. This configuration yields an overall fiber composition of approximately 50% 15D and 50% 3D by mass, identical to that of the uniform control samples, ensuring a true one-to-one comparison. This layered assembly served as the foundation for the continuous gradient formed during the bonding stage.
- **Needle-Punching Consolidation:** The unbonded, layered batt was then transported to a DILO needle-

punching loom for mechanical consolidation. Needle-punching is a process in which a bed of barbed needles is repeatedly pushed through the fibrous batt. As the needles penetrate and withdraw, their barbs catch fibers from the upper layers and entangle them with fibers in the lower layers. This action provides Z-direction fiber reinforcement, physically locking the layers together and densifying the structure. The key effect of this process is the blurring of discrete layer interfaces, creating a continuous, monolithic composite where the fiber composition and, consequently, the density, change gradually through the thickness. The needle board was equipped with 15 × 18 × 36 × 3.5 R/SP triangular barbed needles. To ensure consistent mechanical bonding, the machine was operated at a constant punching density of 200 punches/cm². The needle penetration depth was precisely controlled between 8 mm and 14 mm to achieve the desired final thicknesses for the different samples. The target area densities (1,200, 1,600, and 1,800 g/m²) were achieved by precisely controlling the initial mass of the unbonded batt fed into the machine. For each area density, the final target thicknesses (15, 20, and 25 mm) were achieved by carefully adjusting the needle penetration depth; a lower penetration depth resulted in a thicker, less compacted sample, while a greater depth produced a thinner, more densified sample.

A comprehensive set of nine gradient composite samples was produced, covering three levels of area density (1,200, 1,600, and 1,800 g/m²) and three levels of thickness (15, 20, and 25 mm). For robust comparative analysis, a parallel set of nine uniform-density control samples was also fabricated to the exact same area densities and thicknesses. These control samples were made from a homogeneous 50/50 blend of 3D and 15D fibers.

Characterization and Performance Testing

A suite of standardized tests was employed to characterize the physical and acoustic properties of the fabricated samples.

- **Physical Properties:** The thickness of each sample was measured under a specified pressure (0.5 kPa) using a digital thickness gauge, following ASTM D5729. For each of the nine gradient and nine uniform sample conditions, three replicate samples ($n = 3$) were fabricated. For physical property characterization, at least ten measurements were taken across each replicate sample and averaged. The area density (g/m²) was determined by weighing precisely cut specimens (200 mm × 200 mm) on a calibrated analytical balance. The bulk density (ρ), a crucial parameter in acoustic modeling, was then calculated as the ratio of the area density to the thickness.

- **Airflow Resistance:** The opposition a material presents to the passage of air is a dominant factor influencing sound absorption. This is characterized by two key parameters: airflow resistivity and airflow resistance. Airflow resistivity, σ (in Pa·s/m²), is an intrinsic property of a porous material. For a sample of a given thickness, *t*, the airflow resistance, R (in Pa·s/m), is calculated as $R = \sigma \cdot t$. In this study, the airflow resistance (R) of each composite sample was measured directly using a custom-built apparatus compliant with ASTM C522-03. The airflow resistance is calculated as $R = \Delta P/v$, where ΔP is the pressure difference (Pa) and v is the air velocity (m/s).
- **Acoustic Performance Measurement:** The normal incidence sound absorption coefficient, α, representing the fraction of incident sound energy absorbed by the material, was measured over a wide frequency range. For each condition, three distinct samples were tested. Each sample was removed and repositioned in the impedance tube five times to ensure measurement consistency, and the resulting absorption curves were averaged. The measurements were conducted using a Brüel & Kjær Type 4206 two-microphone impedance tube, strictly following ASTM E1050-12. To cover the frequency range of 100 Hz to 6,300 Hz, two tube configurations with corresponding sample diameters were used: a 100 mm diameter tube for the low-to-mid frequency range (100–1,600 Hz) and a 29 mm diameter tube for the mid-to-high frequency range (800–6,300 Hz). Prior to testing, all samples were conditioned for 24 hours in the testing environment to ensure thermal and hygroscopic equilibrium. The measurements were conducted under standard laboratory conditions (22 ± 2 °C and 50 ± 5% relative humidity). This method is based on measuring the standing wave pattern in the tube, from which the complex reflection coefficient of the sample at the end of the tube is calculated. The sound absorption coefficient is then derived as $\alpha = 1 - |r|^2$, where r is the complex reflection coefficient. The samples were cut with high precision to ensure a snug fit in the holder, preventing edge leaks. All samples were tested with a rigid, impervious backing, simulating a typical wall-mounted installation.
- **Single-Number Rating:** To provide a simple metric for overall performance, the Noise Reduction Coefficient (NRC) was calculated for each sample. The NRC is the arithmetic average of the sound absorption coefficients measured at the one-third octave band center frequencies of 250 Hz, 500 Hz, 1,000 Hz, and 2,000 Hz, rounded to the nearest 0.05.

For clarity, fiber linear density is reported in *denier* throughout (conversion for reference: 1 dtex ≈ 0.9 denier).

Acoustic Modeling and Inverse Characterization

To investigate the theoretical consistency between the experimental performance and the intended gradient design, a numerical fitting procedure based on the Johnson-Champoux-Allard (JCA) model was employed. The gradient sample (G-1600-20) was modeled as a stack of ten thin virtual layers using the Transfer Matrix Method. Since airflow resistivity is the dominant parameter controlling absorption in this context, other JCA parameters (porosity ϕ, tortuosity α_∞, characteristic lengths λ, λ') were estimated using empirical relations for fibrous media (e.g., Garai-Pompoli models) based on the local fiber diameter and bulk density, or held constant to reduce the risk of overfitting.

An optimization algorithm was then used to determine the airflow resistivity profile through the material's thickness that would yield a theoretical sound absorption curve best matching the experimentally measured data. This approach enables the theoretical deduction of the material's internal property gradient based on its macroscopic acoustic performance.

RESULTS

The experimental results provide a quantitative evaluation of the acoustic and physical properties of the gradient density nonwoven composites. The data are presented to systematically illustrate the influence of key structural parameters and to highlight the advantages of the gradient design.

Physical Properties and Airflow Resistance

The measured physical properties, including thickness, bulk density, and airflow resistance, are summarized in Table 1 for the core set of 1,600 g/m² samples. The data show a direct correlation between structural parameters and measured airflow resistance (R_s). For the gradient samples, as thickness increases from 15 mm to 25 mm at a constant area density, the bulk density decreases. Consequently, the airflow resistance also decreases from 14,850 to 8,900 Pa·s/m, because the fibrous network becomes less compact. The uniform sample, at 20 mm thickness, exhibits a significantly higher airflow resistance (18,200 Pa·s/m) than its gradient counterpart (12,100 Pa·s/m). A key, and perhaps counterintuitive, finding is that the gradient composite (G-1600-20) exhibits a significantly lower airflow resistance (12,100 Pa·s/m) than its uniform counterpart (U-1600-20, 18,200 Pa·s/m), despite identical overall composition, mass, and thickness. A two-sample t-test confirmed that the differences in airflow resistance and NRC between the gradient and uniform samples are statistically significant ($p < 0.05$). This difference does not stem from one layer dominating the measurement, but rather from the distinct final microstructures created by the two manufacturing approaches. In the uniform sample, the fine, high-resistance 3D fibers are homogeneously distributed throughout the entire volume, creating a consistently tortuous and restrictive pore network from the front surface to the back, leading to a high overall resistance value. Conversely, in the gradient sample, the effect of the fine 3D fibers is concentrated in the back layer. While this back layer is very dense, the overall structure, with its highly open and non-restrictive frontal section, results in a lower total airflow resistance when measured as a bulk property. The homogeneous distribution of fine fibers in the uniform sample is simply a more effective arrangement for impeding airflow across the composite's full thickness.

Table 1. Physical Properties of Samples with Area Density of 1,600 g/m²

Sample ID	Structure	Thickness (mm)	Bulk Density (kg/m³)	Airflow Resistance (σ, Pa·s/m²)	NRC
G-1600-15	Gradient	15.1 ± 0.2	106.0	14,850 ± 450	0.70
G-1600-20	Gradient	20.2 ± 0.3	79.2	12,100 ± 380	0.75
G-1600-25	Gradient	25.3 ± 0.3	63.2	8,900 ± 310	0.90
U-1600-20	Uniform	20.1 ± 0.2	79.6	18,200 ± 510	0.65

Note: "G" denotes Gradient, "U" denotes Uniform. Data include mean ± standard deviation where appropriate.

Effect of Area Density on Sound Absorption

The effect of area density on the sound absorption coefficient of the gradient composites was investigated while keeping the thickness constant at 20 mm. The absorption curves for samples with area densities of 1,200, 1,600, and 1,800 g/m² are plotted in Figure 1. A clear trend is observable: as the area density increases from 1,200 to 1,600 g/m², the sound absorption performance improves across nearly the entire frequency spectrum, especially in the crucial 400 Hz to 2,000 Hz range. The absorption peak becomes broader and its maximum value increases. This improvement is attributed to the increased amount of fibrous material per unit volume, which enhances the viscous damping effect.

However, a further increase in area density to 1,800 g/m² yields mixed results. While the absorption at lower frequencies (250 Hz to 500 Hz) shows a clear improvement due to the increased mass, the performance in the high-frequency range (above 2,000 Hz) shows a noticeable decline. This indicates that the 1,800 g/m² sample has become too dense, and its surface impedance too high, causing more sound to be reflected rather than absorbed at shorter wavelengths. The 1,600 g/m² sample represents the optimal balance for this thickness, achieving excellent broadband absorption without becoming acoustically reflective at high frequencies.

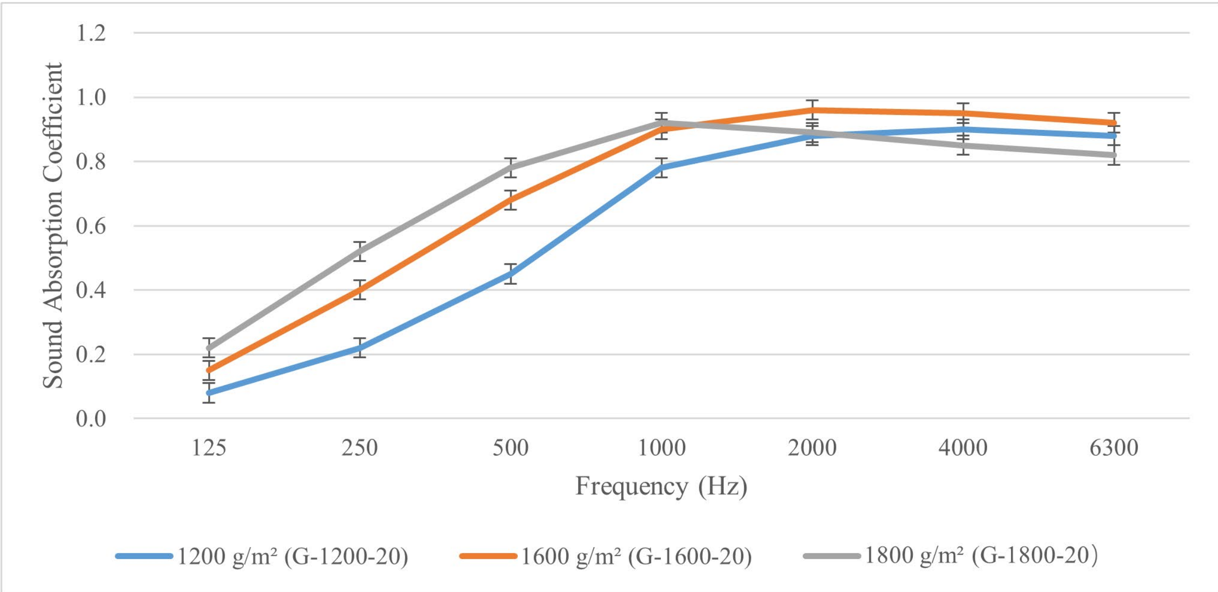

Figure 1. Effect of Area Density on Sound Absorption Coefficient (Thickness = 20 mm)

Effect of Thickness on Sound Absorption

Thickness is arguably the most critical parameter influencing low-frequency sound absorption. Figure 2 illustrates this effect for gradient samples with a fixed area density of 1,600 g/m² and thicknesses of 15, 20, and 25 mm. The results are unequivocal: increasing the thickness leads to a substantial improvement in sound absorption at low and mid frequencies. The first major absorption peak, which corresponds to the quarter-wavelength resonance where the material thickness is approximately λ/4, systematically shifts to lower frequencies as thickness increases. For example, at 500 Hz, the absorption coefficient rises from 0.52 for the

15 mm sample to 0.65 for the 20 mm sample, and further to 0.78 for the 25 mm sample. This demonstrates a direct and powerful relationship between material thickness and its ability to control low-frequency sound, a key challenge in the acoustics of music spaces. At frequencies above 1,500 Hz, all three samples perform exceptionally well, with absorption coefficients approaching unity.

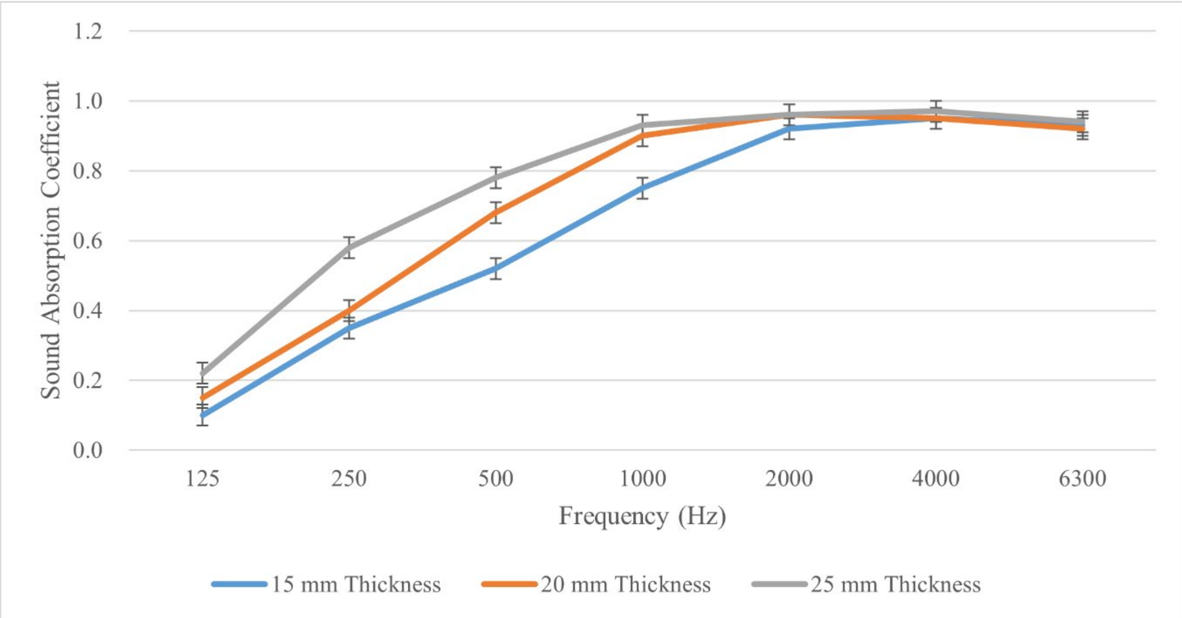

Figure 2. Effect of Thickness on Sound Absorption Coefficient (Area Density = 1,600 g/m²)

Comparative Analysis: Gradient vs. Uniform Structure

The ultimate validation of the gradient design concept comes from a direct comparison with a conventional uniform structure. Figure 3 presents the absorption curves for the optimized gradient sample (G-1600-20) and its uniform counterpart (U-1600-20), which have identical area density, thickness, and overall fiber composition. The superiority of the gradient structure is immediately apparent. Across the critical frequency range from 400 Hz to 3,000 Hz, the gradient sample consistently exhibits a higher sound absorption coefficient. The difference is most pronounced in the 500–1,000 Hz octave bands, which are fundamental to the richness and clarity of music. At 800 Hz, the gradient sample achieves an absorption coefficient of 0.82, while the uniform sample reaches only 0.70. This significant improvement confirms that the strategic arrangement of fibers in the gradient structure leads to a more efficient sound absorption mechanism. The calculated NRC values further quantify this advantage: the gradient sample achieves an effective 0.75, whereas the uniform sample scores a more moderate 0.65 (as shown in Table 1).

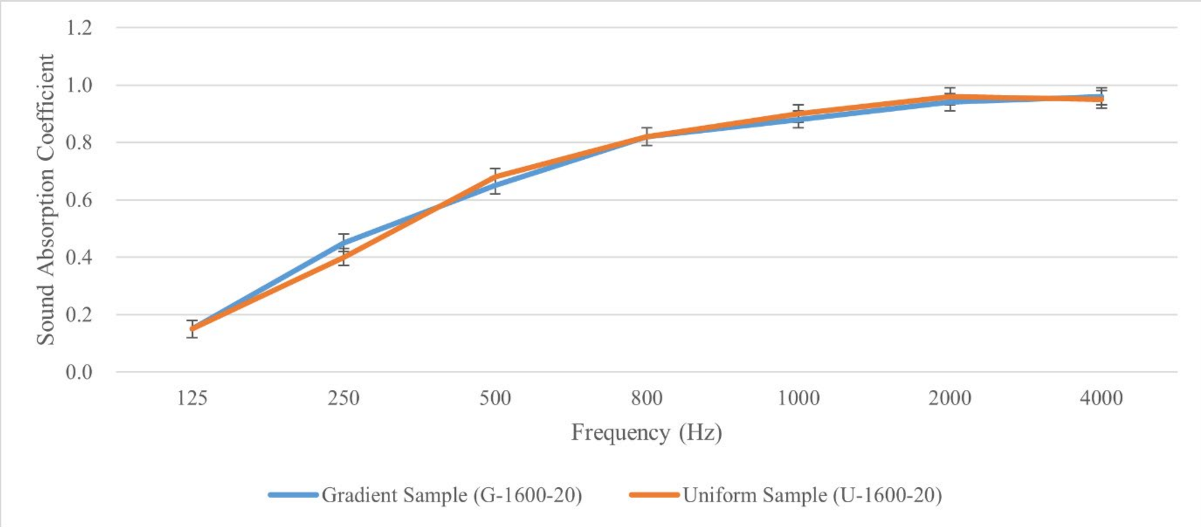

Figure 3. Comparison of Gradient and Uniform Density Structures (1,600 g/m², 20 mm)

Theoretical Analysis of the Gradient Structure via Inverse Modeling

The existence of an effective acoustic gradient was further confirmed through inverse modeling. As shown in Figure 4a, the JCA model, optimized with a gradient profile for airflow resistivity, achieves an excellent fit with the experimental absorption data for the G-1600-20 sample. The specific airflow resistivity profile required to achieve this fit is plotted in Figure 4b. The model predicts a low resistivity (approx. 4,500 Pa·s/m²) at the sound-incident surface, which increases in a quasi-exponential manner to a high value (approx. 25,000 Pa·s/m²) at the back layer. While it is acknowledged that inverse solutions can be non-unique without invasive slicing measurements, this effective resistivity profile is consistent with the physical layering of the manufactured composite, demonstrating that the gradient design concept is theoretically sound.

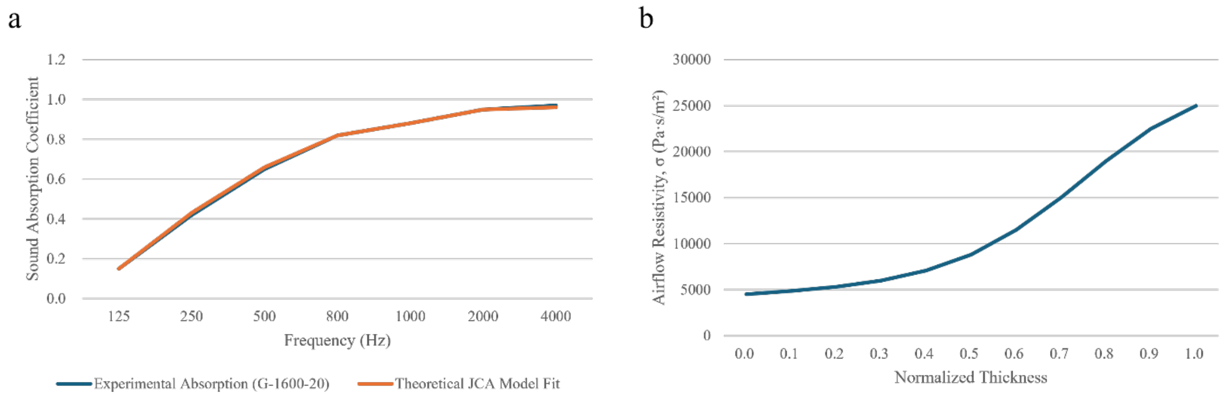

Figure 4. Theoretical Validation of the Gradient Structure. (a) Comparison between the experimentally measured sound absorption coefficient for the G-1600-20 sample and the theoretical prediction from the optimized Johnson–Champoux–Allard (JCA) model, demonstrating an excellent fit. (b) The corresponding airflow resistivity profile predicted by the inverse JCA model, showing a quasi-exponential increase from the sound-incident side (normalized thickness = 0) to the back layer (normalized thickness = 1)

DISCUSSION

The comprehensive experimental results presented in this study provide strong evidence supporting the acoustic efficacy of a gradient density design for nonwoven sound absorbers. A deeper analysis of these results, interpreted through the lens of acoustic theory and material science, reveals the underlying mechanisms responsible for the observed performance enhancements and offers valuable insights for practical application.

The core of the gradient concept's success lies in its ability to engineer a more favorable acoustic impedance profile. According to the classical Delany-Bazley-Miki model for porous materials, the characteristic impedance (Zc) and propagation constant (k) are complex functions of the material's airflow resistivity. A large impedance mismatch between the air and the material surface causes a significant portion of the incident sound wave to be reflected. The uniform sample (U-1600-20) has a relatively high airflow resistance of 18,200 Pa·s/m². This high resistance, while beneficial for internal energy dissipation, also contributes to a higher surface impedance, leading to reflection, particularly as frequency increases. In contrast, the gradient sample (G-1600-20), despite having the same mass, presents a much lower overall airflow resistivity of 12,100 Pa·s/m². This is because its front layer, composed of coarse 15D fibers, is highly porous and has very low resistivity. This layer acts as an effective impedance-matching interface, coaxing the sound wave into the material with minimal reflection. This is analogous to an anti-reflection coating in optics.

Once the sound wave has penetrated the material, the gradient structure ensures its efficient attenuation. As the wave propagates deeper, it encounters a medium of progressively increasing density and airflow resistance due to the increasing concentration of fine 3D fibers. This gradual increase in resistance ensures that the sound energy is continuously and efficiently converted into heat via viscous and thermal losses throughout the material's thickness, rather than being dissipated abruptly in a thin surface layer. This distributed damping mechanism is what leads to the broader and higher absorption curve observed in Figure 3. The uniform material, lacking this structural sophistication, represents a compromise: its single density value is too high for optimal impedance matching at the surface and may not be optimally distributed for dissipation throughout its depth.

The superiority of the gradient structure at lower frequencies can be understood more deeply by analyzing its interaction with long-wavelength sound waves in the context of the quarter-wavelength principle. For low-frequency sound, the point of maximum air particle velocity—and thus the point of maximum potential for frictional losses—occurs at a significant distance from the rigid backing ($\lambda/4$). A material's effectiveness at these frequencies is therefore determined by its ability to both allow sound to penetrate deep into its structure and then provide high resistance to airflow at that optimal depth. Herein lies the specific advantage of the engineered fiber arrangement:

- The frontal layer, composed of coarse 15D fibers, creates a lofty, highly porous structure with low airflow resistance. Its primary role for low-frequency waves is not absorption, but to act as an acoustically transparent entry gate, allowing the long-wavelength energy to penetrate deep into the composite with minimal surface reflection.
- The back layer, composed of fine 3D fibers, creates a dense, tortuous network with a high surface area and, consequently, high airflow resistance. This layer is the engine of low-frequency dissipation. It is strategically positioned deeper within the composite, where the particle velocity of the penetrating low-frequency wave is highest, thereby maximizing the conversion of acoustic energy into heat through viscous friction.

A uniform material, by contrast, presents a fundamental compromise. If it is dense enough to be effective at dissipating energy deep within its structure, its surface impedance is often too high, causing initial reflection of low-frequency waves. If it is open enough to allow sound to penetrate, it lacks the high-density fibrous network deep inside to effectively damp the wave. The gradient structure resolves this compromise by creating a specialized, dual-function material: it combines a low-resistance entry zone with a high-dissipation core, effectively extending its absorptive efficiency into the challenging low-frequency spectrum.

The systematic investigation of area density and thickness further refines our understanding. The existence of an optimal area density (1,600 g/m² for a 20 mm thickness) confirms the well-established principle that for any given thickness, there is an optimal range of airflow resistance. The performance drop of the 1,800 g/m² sample at high frequencies is a classic example of a material becoming too acoustically hard. The powerful effect of thickness on low-frequency performance (Figure 2) is a direct manifestation of the quarter-wavelength principle. A sound absorber is most effective when its thickness is a significant fraction of the sound's wavelength. By increasing the thickness from 15 mm to 25 mm, we directly extend the material's effective absorption range to lower frequencies, which is a critical consideration for broadband acoustic control.

From a practical standpoint, the optimized G-1600-20 sample represents a highly compelling solution for music spaces. With an NRC of 0.75, it demonstrates highly effective sound absorption for a thin-profile material. Its performance is particularly strong in the 500–4,000 Hz range. This broad bandwidth suggests the material could be effective in reducing excessive sound energy in critical frequency bands without relying on thick, heavy structures. The fact that this superior performance is achieved simply by the intelligent arrangement of fibers, without resorting to exotic materials or complex multi-component assembly, makes it a cost-effective and scalable manufacturing proposition. The study is, however, subject to certain limitations. The comparison was made against a uniform control sample to isolate the effect of the gradient structure, but a comprehensive benchmark against industry-standard materials such as mineral wool or fiberglass was not performed. Such a comparative analysis is a critical next step to fully establish the material's practical and commercial relevance. Furthermore, the current work is limited to normal incidence sound absorption. In real-world architectural scenarios, sound arrives from all angles. Future research should therefore include diffuse-field sound absorption measurements in a reverberation chamber to provide a more complete picture of the material's performance. Nonetheless, the normal incidence data provide a robust and fundamental characterization of the material's intrinsic absorptive capabilities and clearly validate the scientific merit of the gradient density design philosophy.

CONCLUSION

In this research, a novel gradient density nonwoven composite material was successfully designed, fabricated, and optimized for high-performance sound absorption through microstructural engineering. Through a systematic approach involving the layering of polyester fibers with different deniers followed by needle-punching consolidation, a monolithic structure was created with a continuous gradient in its physical properties. This design moves beyond simple homogeneous or discrete multi-layer structures, offering a more sophisticated method for controlling the interaction of sound with fibrous media.

The comprehensive experimental investigation yielded several key conclusions. First, the gradient density structure unequivocally outperforms a conventional uniform structure of identical mass, thickness, and composition, demonstrating significantly higher normal incidence sound absorption coefficients in the critical mid-to-high frequency range and achieving a higher overall NRC of 0.75 compared to 0.65. This superior performance is directly attributed to the engineered impedance gradient, which enhances sound transmission into the material while maximizing internal energy dissipation. Second, the study established clear relationships between the material's structural parameters and its acoustic performance. An optimal area density of 1,600 g/m² (for a 20 mm thickness) was identified, and the profound impact of thickness on low-frequency absorption was quantitatively confirmed. These findings provide essential design guidelines for tailoring the material to specific acoustic targets.

Ultimately, this work validates a powerful design principle for advanced acoustic textiles. The developed gradient nonwoven composite demonstrates a scientifically robust design strategy. Its superior normal incidence performance indicates that the material is a promising candidate for controlling reverberation in music halls, recording studios, and other critical listening environments, pending further diffuse-field validation. It contributes to the field of technical textiles by demonstrating how microstructural engineering can be leveraged to achieve significant gains in functional performance. Future research should extend this concept by performing a comprehensive benchmarking study against commercially available acoustic materials, exploring different fiber materials (e.g., natural fibers for enhanced sustainability), investigating the integration of resonant structures such as micro-perforated membranes to further target low-frequency absorption, and conducting diffuse-field acoustic characterization to fully validate its performance in real-world architectural applications.

Availability of Data and Materials

The datasets used and analysed during the current study were available from the corresponding author on reasonable request.

Author Contributions

Fei Mo designed, collected and analyzed the data, and drafted the manuscript. Fei Mo conducted the study, critically revised the manuscript for important intellectual content, and gave final approval of the version to be published. Fei Mo participated fully in the work, take public responsibility for appropriate portions of the content, and agreed to be accountable for all aspects of the work in ensuring that questions related to the accuracy or integrity of any part of the work are appropriately investigated and resolved.

Acknowledgments

Not applicable.

Funding

Study on the Application Model of Red Opera inVocal Music Teaching in Local Universities. (Grant No. 23DSSK004).

Conflict of Interest

The author declares no conflict of interest.

REFERENCES

[1] Long M. Architectural Acoustics. New York, NY, USA: Elsevier; 2005. eBook ISBN: 9780080527550.

[2] Beranek LL. Concert Halls and Opera Houses: Music, Acoustics, and Architecture. Berlin/Heidelberg, Germany: Springer; 2004.

[3] Barron M. Auditorium Acoustics and Architectural Design. Abingdon, UK: Spon Press; 2009. doi: 10.4324/9780203874226

[4] Everest FA. Master Handbook of Acoustics. New York, NY, USA: McGraw-Hill Education; ISBN: 9781260473605. 2022.

[5] Crocker MJ. Handbook of Noise and Vibration Control. Hoboken, NJ, USA: John Wiley & Sons; 2007. doi: 10.1121/1.2973236

[6] Jang E-S. Sound absorbing properties of selected green material—A review. Forests. 2023; 14(7):1366. doi: 10.3390/f14071366

[7] Yang T, Saati F, Horoshenkov KV, Xiong X, Yang K, Mishra R, et al. Study on the sound absorption behavior of multi-component polyester nonwovens: Experimental and numerical methods. Textile Research Journal. 2019; 89(16):3342-3361. doi: 10.1177/0040517518811940

[8] Al-Maharma AY, Al-Huniti N. Critical review of the parameters affecting the effectiveness of moisture absorption treatments used for natural composites. Journal of Composites Science. 2019; (1):27. doi: 10.3390/jcs3010027

[9] Mouritz AP, Bannister MK, Falzon P, Leong K. Review of applications for advanced three-dimensional fibre textile composites. Composites Part A: Applied Science and Manufacturing. 1999; 30(12):1445-1461. doi: 10.1016/S1359-835X(99)00034-2

[10] Pierce AD. Acoustics: An Introduction to Its Physical Principles and Applications. Berlin/Heidelberg, Germany: Springer; 2019.

[11] Asdrubali F, Schiavoni S, Horoshenkov K. A review of sustainable materials for acoustic applications. Building Acoustics. 2012; 19(4):283-311. doi: 10.1260/1351-010X.19.4.28

[12] Salehi F, Jamshidi Avanaki M, Nouri M. An investigation into the designing of fibrous sound absorption materials incorporated with nanofibers: A case study of a multi-layered material composed of PET nonwoven and PAN nanofibers. The Journal of The Textile Institute. 2022; 113(9):1816-1825. doi: 10.1080/00405000.2021.1950443

[13] Zhu J, Sun J, Tang H, Wang J, Ao Q, Bao T, et al. Gradient-structural optimization of metal fiber porous materials for sound absorption. Powder Technology. 2016; 301:1235-1241. doi: 10.1016/j.powtec.2016.08.006